

Ventilation Mechanisms of Deep Water in the Sulu Sea

Yanagi, Tetsuo

Research Institute for Applied Mechanics, Kyushu University

Miyamoto, Hideki

Department of Earth System Science and Technology, Interdisciplinary Graduate School of Engineering Sciences, Kyushu University

Gamo, Toshitaka

Ocean Research Institute, University of Tokyo

Hasumoto, Hiroshi

Ocean Research Institute, University of Tokyo

<https://doi.org/10.15017/26834>

出版情報：九州大学応用力学研究所所報. 133, pp.71-79, 2007-09. Research Institute for Applied Mechanics, Kyushu University

バージョン：

権利関係：

Ventilation Mechanisms of Deep Water in the Sulu Sea

Tetsuo YANAGI*¹, Hideki MIYAMOTO*², Toshitaka GAMO*³
and Hiroshi HASUMOTO³

E-mail of corresponding author: yanagi@riam.kyushu-u.ac.jp

(Received June 4, 2007)

Abstract

Ventilation mechanisms of the deep water in the Sulu Sea, which is a deep marginal sea (maximum depth of about 5,000 m) with a shallow sill (depth of about 400 m) at low latitude in the western Pacific Ocean, was discussed based on the analysis of historical data and a simple numerical experiment. The observed changes in vertical profiles of potential water temperature, salinity and potential density between 1996 and 2002 in the deepest part of the Sulu Sea were well reproduced by a simple numerical experiment. The heavy water mass was uplifted from the lower layer near the Mindoro Strait in the South China Sea due to the development of an anti-cyclonic gyre and the passing of a typhoon in autumn, and subducted from 400 m depth of the South China Sea to 5,000 m depth of the Sulu Sea in 5 days. The terrestrial heat flow from the sea bottom played an important role in the ventilation of deep water in the Sulu Sea. The average residence time, up to about 300 years, of deep water in the Sulu Sea was explained by the large vertical diffusivity of $10 \text{ cm}^2 \text{ s}^{-1}$ in the deep water of the Sulu Sea, which might be resulted from the propagation of internal wave energy from the upper layer.

Key words : *deep water ventilation, terrestrial heat flow, Sulu Sea, large vertical diffusivity in the deep water, internal wave*

1. Introduction

There are many marginal seas in the western Pacific Ocean, such as the Bering Sea at the northern end and the Tasmania Sea at the southern end. Among these marginal seas, the characteristics of the deep water in the Sulu Sea are unique. The Sulu Sea is a semi-enclosed sea with a shallow sill of about 400 m deep and the deepest part of about 5,000 m as shown in Fig.1, and the deep water in the Sulu Sea is very warm and has a low dissolved oxygen concentration.

There is no direct ventilation mechanism of the deep water in the Sulu Sea such as winter convection, because it is located at low latitude. Quadfasel *et al.*(1990)¹⁾ claimed that the deep water in the Sulu Sea was ventilated by a turbidity current, which was induced by the change in water density that resulted from sediment influx. They

stated that this turbidity current was triggered by the uplift of the heavy water mass in the South China Sea, possibly due to the passage of a severe typhoon, and had been generated at intervals of several decades, as indicated by the frequent deposition of graded sequences of silty mud on the abyssal plain of the Sulu Sea. However, this proposed mechanism is questionable because the turbidity current can transport the bottom sediment from 400 m depth to 5,000 m depth, but cannot transport the water itself from 400 m depth to 5,000 m depth. The water mass in the turbidity current is changed successively as the turbidity current flows down. The ventilation mechanism of the deep water in the Sulu Sea has not been yet clarified.

In this paper, the ventilation mechanism of the deep water in the Sulu Sea is investigated based on the analysis of historical observed data and a simple numerical experiment.

2. Vertical distribution of potential water temperature, salinity, potential density and dissolved oxygen

*1 Research Institute for Applied Mechanics, Kyushu University

*2 Department of Earth System Science and Technology, Interdisciplinary Graduate School of Engineering Sciences, Kyushu University

*3 Ocean Research Institute, University of Tokyo

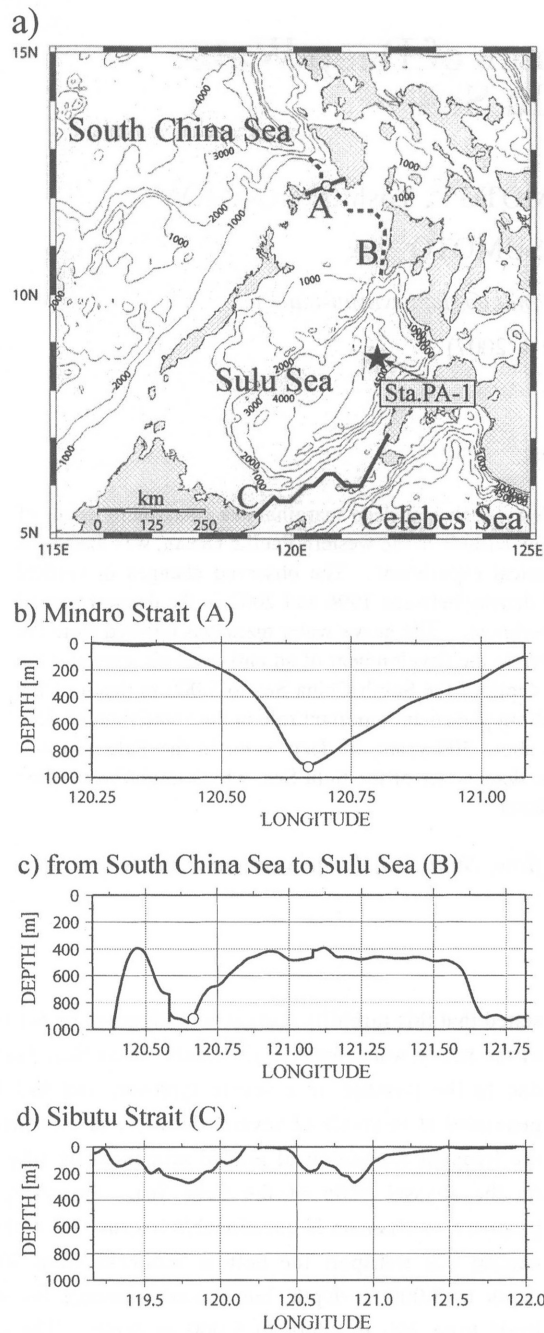


Fig.1 The South China Sea, the Sulu Sea and the Celebes Sea, where numbers show the depth in meters (a). The bottom topography across the Mindoro Strait (b), that from the South China Sea to the Sulu Sea (c), and that across the Sibutu Strait (d). Sta.PA-1 in (a) is the CTD station in 1996 and 2002.

Used data in this study was obtained from the World Ocean Database CD-ROM (Ver 1.2). The vertical distributions of the potential water temperature, salinity, potential density and dissolved-oxygen (DO) concentration along the central section from the South

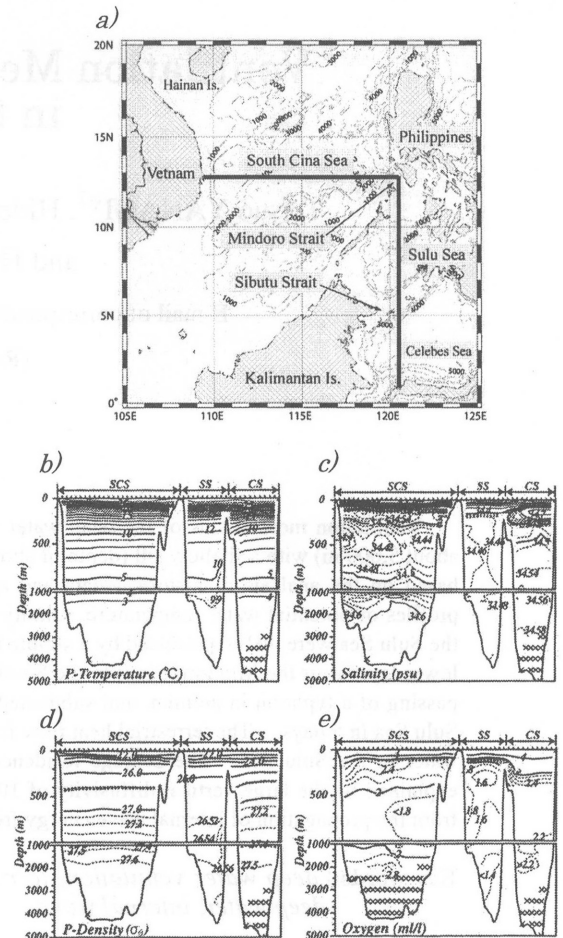


Fig.2 Vertical sections of potential water temperature (b), salinity (c), potential density (d) and dissolved oxygen concentration (e) in the South China Sea, the Sulu Sea and the Celebes Sea along the full line in (a). Crosses show the points where there is no available data.

China Sea to the Celebes Sea are shown in Fig.2. Potential water temperature in the layer below 1,000 m in the Sulu Sea is about 10°C and it is much higher than those in the same layers of the South China Sea and the Celebes Sea, which are about 3 °C~4°C as shown in Fig.2 (b). Salinity and potential density in the deep layer of the Sulu Sea are lower than those in the same layers of the South China Sea and the Celebes Sea as shown in Fig.2 (c) and (d). DO concentration in the deep layer of the Sulu Sea is very low compared to those in the South China Sea and the Celebes Sea as shown in Fig.2 (e). These facts suggest that the deep water in the Sulu Sea is ventilated by the subduction of warm and less saline sub-surface water in the South China Sea or the Celebes Sea, and the average residence time of the deep water in the Sulu Sea is rather long.

The Sulu Sea connects to the South China Sea through a narrow passage of the Mindoro Strait, whose deepest part is about 900 m as shown in Fig.1 (b), but

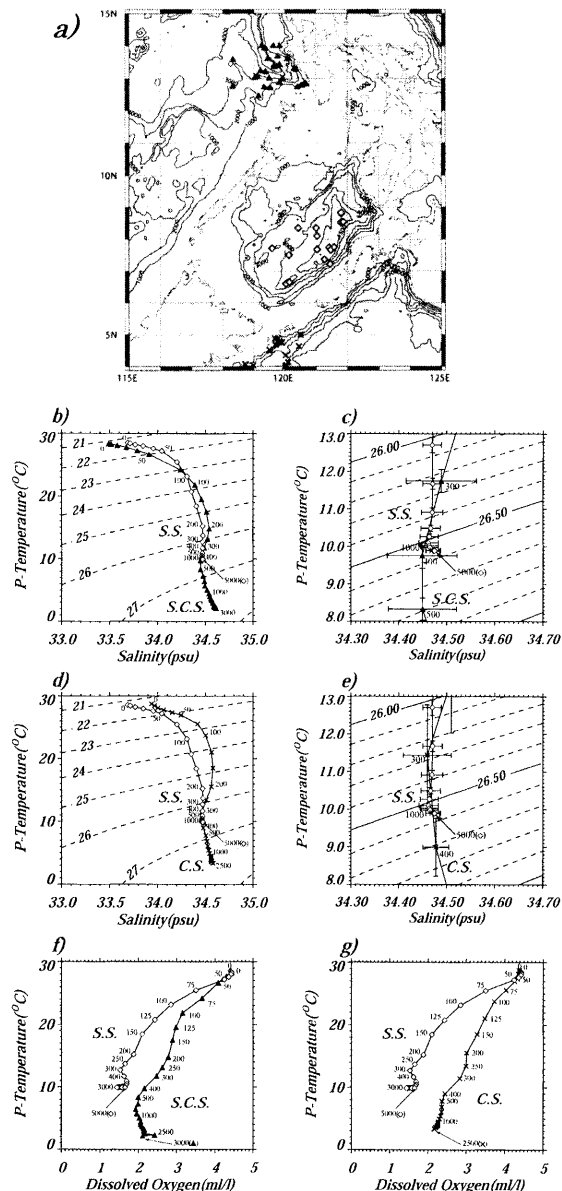


Fig.3 Potential water temperature and salinity diagrams in the western part of the South China Sea near the Mindoro Strait (S.C.S.) (averaged at stations shown by full triangles in (a)) and in the Sulu Sea (S.S.) (averaged at stations shown by open diamonds in (a)) (b), and its expansion of the deeper part (c). Those in the Sulu Sea and in the northwestern part of the Celebes Sea near the Sibutu Strait (C.S.) (average at stations shown by crosses in (a)) (d), and its expansion in the deeper part (e). Horizontal and vertical bars in (c) and (e) show the standard deviation. Potential water temperature and DO diagrams in the South China Sea and in the Sulu Sea (f) and those in the Sulu Sea and the Celebes Sea (g).

the sill depth from the South China Sea to the Sulu Sea is about 400 m as shown in Fig.1 (c). The Sulu Sea also connects to the Celebes Sea through the southern passage of the Sibutu Strait whose sill depth is about 300 m as shown in Fig.1 (d).

3. Potential water temperature - salinity and potential water temperature - DO diagrams

The potential water temperature and salinity diagrams of the Sulu Sea (averaged at stations shown by open diamonds in Fig.3 (a)) and the eastern part of the South China Sea near the Mindoro Strait (averaged at stations shown by full triangles in Fig.3 (a)) are shown in Figs.3 (b) and (c). Potential water temperature, salinity and potential density at 5,000 m depth of the Sulu Sea are nearly the same as those at 400 m depth in the South China Sea, and the water mass at 400 m depth in the South China Sea is heavier or lighter than that at 5,000 m depth in the Sulu Sea as shown by the standard deviation in Fig.3 (c). The potential water temperature and salinity diagrams of the Sulu Sea and the northwestern part of the Celebes Sea near the Sibutu Strait (averaged at stations shown by crosses in Fig.3 (a)) are shown in Figs.3 (d) and (e). Potential density of the water mass at 5,000 m depth in the Sulu Sea is higher than that at 300 m depth in the Celebes Sea as shown in Fig.3 (e). These results suggest that the deep water in the Sulu Sea is ventilated not by the water mass at 300 m depth of the Celebes Sea but by that at 400 m depth of the South China Sea. The ventilation is sporadic because DO concentration at 5,000 m depth in the Sulu Sea is lower than that at 400 m depth in the South China Sea as shown in Fig.3 (f). It is also lower than that at 300 m depth in the Celebes Sea as shown in Fig.3 (g). Nozaki et al. (1999)²⁾ claimed that the average residence time of the deep water in the Sulu Sea was 300 ± 150 years from the observed data of $\Delta^{14}\text{C}$ and DO.

4. Seasonal variation in water characteristic at 400 m depth in the South China Sea and at 5,000 m depth in the Sulu Sea

Seasonal variations in potential water temperature, salinity, potential density, and DO at 400 m depth in the eastern part of the South China Sea near the Mindoro Strait (averaged at stations shown by full triangles in Fig.3 (a)) and those averaged between 3,000 m and 5,000 m depths in the Sulu Sea (averaged at stations shown by open diamonds in Fig.3 (a)) are shown in Fig.4.

Those at 5,000 m depth in the Sulu Sea are nearly constant throughout the year, though data is not available for May, July and from November to March.

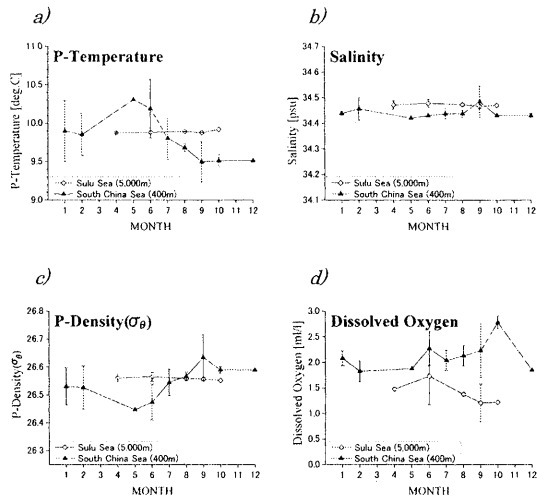


Fig.4 Seasonal variations in potential water temperature (a), salinity (b), potential density (c) and dissolved oxygen (d) at 400 m depth in the South China Sea (averaged at stations shown by full triangle in Fig.3 (a)) and those averaged from 3,000 m to 5,000 m depths in the Sulu Sea (averaged at stations shown by open diamond in Fig.3 (a)). Vertical bars show the standard deviation.

On the other hand, potential water temperature and potential density at 400 m depth in the South China Sea is higher and lower, respectively, than those at 5,000 m in the Sulu Sea in spring, but opposite in autumn (though data is not available for March, April and November). Salinity at 400 m depth in the South China Sea is higher than that at 5,000 m depth in the Sulu Sea in September. These results suggest that the heavy water mass with low water temperature and high salinity may appear at 400 m depth in the eastern part of the South China Sea near the Mindoro Strait in autumn, and it may be possible to have subducted to 5,000 m depth in the Sulu Sea because it is heavier than the deep water of the Sulu Sea (Fig.4 (c)).

The appearance of a heavy water mass at 400 m depth in the eastern part of the South China Sea in autumn is partly due to the seasonal variation in surface circulation of the South China Sea as shown in Fig.5. A cyclonic gyre develops near the Mindoro Strait in spring (Fig.5 (a)), but an anti-cyclonic gyre in autumn (Fig.5 (c)) (Morimoto *et al.*, 2000)³. A cyclonic gyre in the northern hemisphere accompanies the downlifted isopycnal surface at 400 m depth near the Mindoro Strait (Fig.5 (e)), while an anti-cyclonic gyre accompanies the uplifted isopycnal surface (Fig.5 (f)). A cyclonic gyre results in a light water mass in spring, and an anti-cyclonic gyre a heavy water mass in autumn as shown in Fig.4 (c). There is no remarkable gyre near the Mindoro Strait during summer and winter

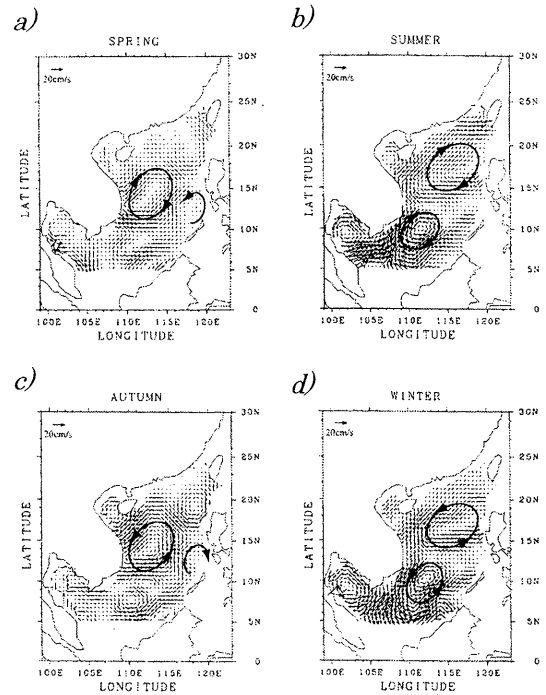


Fig.5 Seasonal variation in the surface circulation of the South China Sea ((a) to (d)) from Morimoto *et al.* (2000) and schematic representation of horizontal and vertical structures of cyclonic (spring, (e)) and anti-cyclonic (autumn, (f)) eddies.

(Figs.5 (b) and (d)). Another reason for the appearance of a heavy water mass at 400 m depth in the South China Sea in autumn is the passing of a typhoon. The tracks of all typhoons passing over the South China Sea from 1950 to 2005 are shown in Fig.6 (a), and the seasonal variation in its frequency is shown in Fig.6 (b) (National Institute of Information ; <http://www.digital-typhoon.org/>). The most frequent typhoon passing over the South China Sea occurs in autumn. The typhoon passing may generate an internal disturbance by uplifting the heavy water mass to 400 m depth near the Mindoro Strait. We may assume that the surface circulation in the South China Sea and the frequent typhoon passing over the South China Sea in

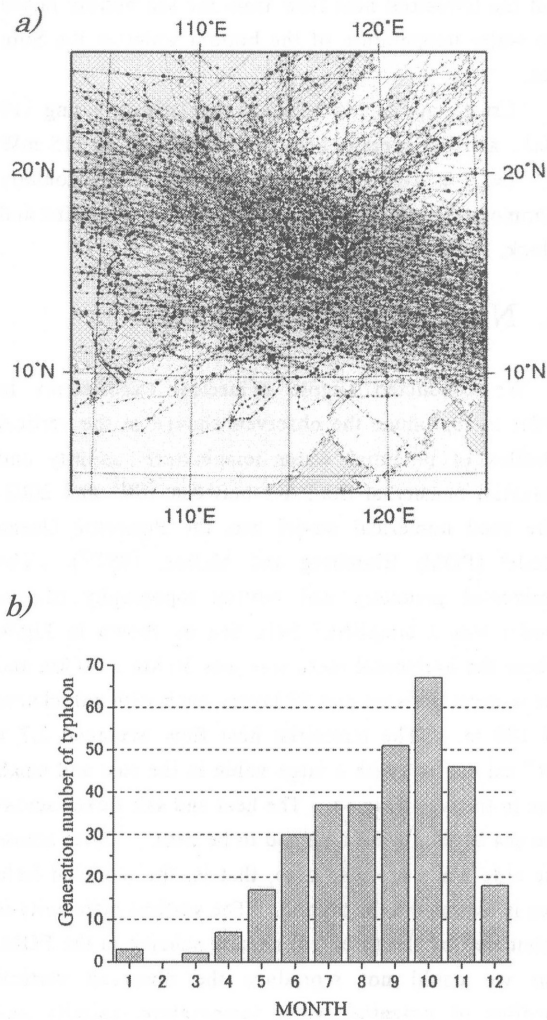


Fig.6 Tracks of typhoons passing over the South China Sea from 1950 to 2005 (a) and the monthly accumulated numbers (b) (<http://www.digital-typhoon.org/>).

autumn may uplift a heavy water mass to the 400 m depth near the Mindoro Strait and trigger the subduction of subsurface water in the South China Sea to the deep layer of the Sulu Sea.

The DO concentration at 400 m depth in the South China Sea is always higher than that at 5,000 m depth in the Sulu Sea (Fig.4 (d)).

5. CTD observations

Figures 7 (a) and (b) show the vertical profiles of potential water temperature, salinity and potential density at Sta.PA-1 (see Fig.1) of the Sulu Sea observed in December 1996 (Nozaki *et al.*, 1999)²⁾ and in December 2002 (Gamo *et al.*, 2003)⁴⁾ using SEABIRD-CTD-911plus. The accuracy of these data

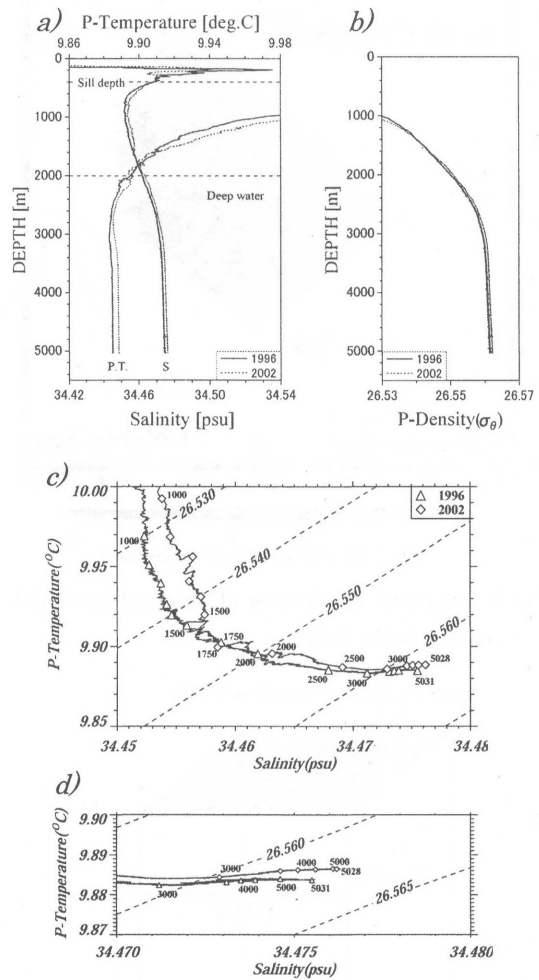


Fig.7 Vertical profiles of potential water temperature and salinity (a), and potential density (b), potential water temperature and salinity diagrams (c) and its expansion deeper than 3,000 m (d) observed at Sta.PA-1 in 1996 and 2002 (Nozaki *et al.*, 1999; Gamo *et al.*, 2003).

is 0.001 °C for water temperature, 0.003 psu for salinity and 0.003 σ_θ for density (Gamo *et al.*, 2003)⁴⁾. The deep water below 2,000 m in 2002 had a higher potential water temperature (0.003 °C), higher salinity (0.002 psu) and higher potential density (0.0007 σ_θ) than in 1996. Only the difference of potential water temperature is significant. This result suggests that the warm, salty and heavier water mass might subduct into the deep layer of the Sulu Sea between 1996 and 2002 because the subducted heavy water mass with higher water temperature must have a higher salinity. Figures 7 (c) and (d) show the potential water temperature – salinity diagrams below 1,000 m depth and that below 3,000 m depth, in 1996 and 2002. The potential water temperature and salinity between 1,500 m and 2,000 m were nearly the same in 1996 and 2002, but those below

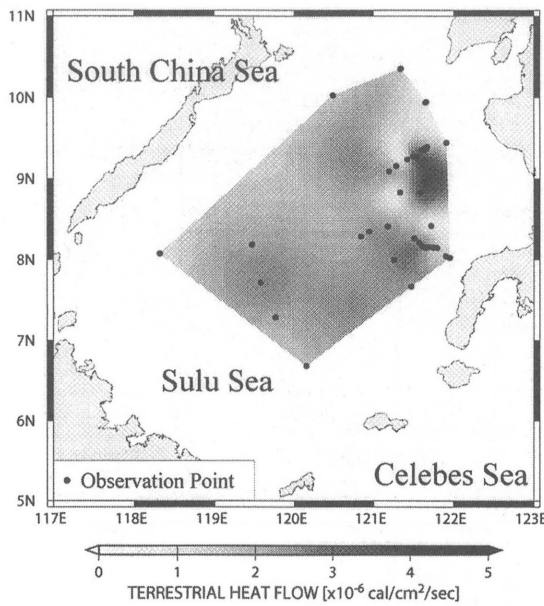


Fig. 8 Horizontal distribution of observed terrestrial heat flow in the Sulu Sea.

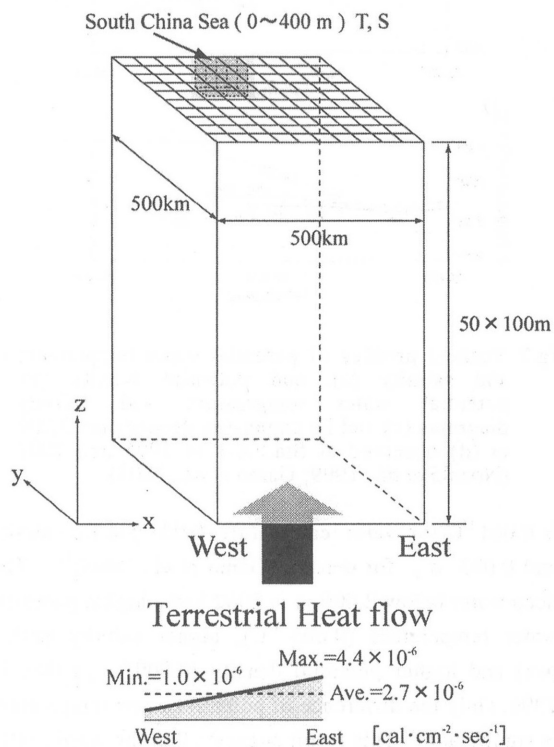


Fig.9 Used numerical model of the simplified Sulu Sea.

2,000 m were different between 1996 and 2002 as shown in Fig.7 (c). We can define the deep water of the Sulu Sea as the water mass below 2,000 m depth from Figs.7 (a) and (c). Potential water temperature at the bottom (9.885°C in 1996 and 9.888°C in 2002) is 0.002°C higher than that at 3,000 m (9.883°C in 1996

and 9.886°C in 2002) (Fig.7 (d)). This result suggests that the terrestrial heat flow from the sea bottom raised the water temperature of the bottom water in the Sulu Sea.

Crustal age of the Sulu Sea is relatively young (19 Ma), and the average heat flow is as high as 115 mW m^{-2} ($=2.7 \times 10^{-6} \text{ cal cm}^{-2} \text{ sec}^{-1}$) with a horizontally inhomogeneous distribution as shown in Fig.8 (Hinz and Block, 1990⁵); Lewis, 1991⁶).

6. Numerical experiments

We conducted simple numerical experiments in order to reproduce the observed change in the vertical profiles of potential water temperature, salinity and potential density at Sta.PA-1 between 1996 and 2002. The used numerical model was the Princeton Ocean Model (POM; Blumberg and Mellor, 1987⁷). The horizontal geometry and bottom topography of our model was a simplified Sulu Sea as shown in Fig.9, where the horizontal mesh size was $50 \text{ km} \times 50 \text{ km}$ and the vertical division was 50 layers, each with a thickness of 100 m. The terrestrial heat flow averaged $2.7 \times 10^{-6} \text{ cal cm}^{-2} \text{ s}^{-1}$ with a large value in the east and small one in the west (Fig.8). The heat and salt fluxes across the sea surface were assumed to be zero. Those across the side walls are also zero, that is, the modeled Sulu Sea is assumed to be a pond. The vertical diffusivity is calculated by the turbulent closure scheme in the POM, but we could not reproduce the observed vertical profiles of potential water temperature, salinity and potential density near the bottom using the vertical diffusivity calculated by the POM. When we gave a background vertical diffusivity of $10 \text{ cm}^2 \text{ s}^{-1}$ below 3,000 m, we could reproduce the vertical profiles of potential water temperature, salinity and potential density near the bottom as shown later.

The observed potential water temperature, salinity and potential density profiles in 1996 were given as an initial condition for the entire area of the modeled Sulu Sea. The heavy water mass of $26.620 \sigma_{\theta}$ (average potential density at 400 m depth of the South China Sea in September as shown in Fig.4 (c)) with larger density than that at 5,000 m depth ($26.562 \sigma_{\theta}$ as shown in Fig.7 (d)) of the Sulu Sea was given at 400 m depth of the modeled South China Sea (shown by the hatched area in Fig.9) in 1 day. The succeeding subduction process was calculated with time steps of 1.0 second for the external mode and 10.0 seconds for the internal mode. The calculation results are shown in Fig.10. The heavy water mass reached the bottom of the Sulu Sea 1 day after the beginning of the calculation, mixed

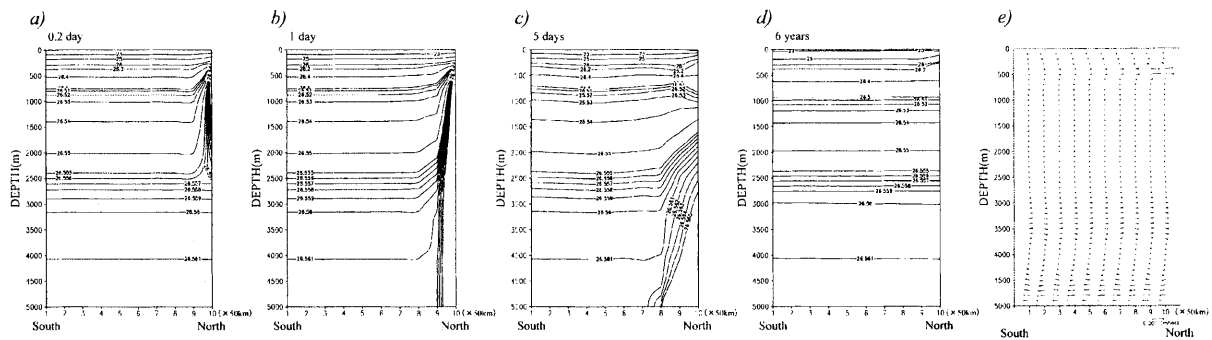


Fig.10 Calculation result on the subduction of heavy water mass from 400 m depth of the South China Sea to the deep layer of the Sulu Sea, where density distribution 0.2 day after the beginning of the calculation (a), that 1 day after the beginning (b), that 5 days after the beginning (c), that 6 years after the beginning (d), and the vertical distribution of current vectors 6 years after the beginning of the calculation (e).

with the deep water below 2,000 m 5 days after the beginning of the calculation and stratified 6 years after the beginning of the calculation as shown in Fig.10 (a) to (d). We confirmed the same result was obtained using a non-hydrostatic numerical model, though it took a much longer calculation time compared to the POM. The vertical circulation due to the terrestrial heat flow shown in Fig.10 (e) plays an important role in the mixing of the deep water below 2,000 m in the Sulu Sea.

After some trial and error, we could reproduce the observed change in vertical profiles of potential water temperature, salinity and potential density between 1996 to 2002 as shown in Figs.7 (a) and (b), by supplying the water mass with potential water temperature of 9.900°C , salinity of 34.500 psu and potential density of $26.579 \sigma_{\theta}$ in 5 days from 400 m depth, as shown in Fig.11. The given salinity and density at 400 m depth in the calculation are within the standard deviation observed at 400 m depth in the South China Sea as shown in Figs.4 (b) and (c), though the given water temperature is a little outside the standard deviation of the observed one as shown in Fig.4 (a). We cannot distinguish the differences between the observations in 1996 and 2002, and between the observation and calculation in the full scale figure from 0 m to 5,000 m as shown in Figs.11 (a) to (c), but their differences are very clear below 2,500 m as shown in Figs.11 (d) to (f).

As shown in Fig.11 (d), 1 day supply of the heavy water mass at 400 m depth of the South China Sea resulted in a lower potential water temperature near the bottom than the observed result but 10 days supply resulted in higher potential water temperature. Five days supply of the heavy water mass gave the best reproduction for potential water temperature, salinity and potential density as shown in Fig.11 (d), (e) and (f). Calculated and observed average water temperature below 2,000 m depth in 2002 was 9.888°C and 9.888

$^{\circ}\text{C}$, respectively. A small discrepancy exists between the calculated and observed vertical profiles of water temperature below 3,000 m depth. We suppose that this is due to a simplification of horizontal geometry and bottom topography of the modeled Sulu Sea. The complicated geometry and topography may induce a complicated convection near the bottom, and result in a vertically homogeneous distribution of potential water temperature near the bottom.

Calculated 5 days subduction does not mean necessarily that the subduction occurred in 5 days in 1996. We could get the similar results from the other experiments with 5 subductions of 1 day supply within 6 years from 1996 to 2002.

The calculation results of 5 days supply of heavy water mass without the terrestrial heat flow are shown in Figs.12 (a) – (c), where the potential water temperature near the bottom is lower than the observed results. This suggests that the terrestrial heat flow plays an important role in the ventilation of the deep water in the Sulu Sea through its effect of heat and buoyancy supply. The calculation result of 5 days supply of heavy water mass with a small vertical diffusivity of $1 \text{ cm}^2 \text{ s}^{-1}$ below 3,000 m is shown in Figs.12 (d) – (f), where the stratification develops near the bottom, and the calculated result greatly differs from the observed result. A large vertical diffusivity of $10 \text{ cm}^2 \text{ s}^{-1}$ below 3,000 m, which is necessary for a good reproduction in our calculation, has not been reported yet from field measurements in the Sulu Sea. However, such a large vertical diffusivity may be possible by the propagation of internal wave energy from the upper layer because an internal wave with a large amplitude as much as 90 m develops at spring tide in the southwestern part of the Sulu Sea (Apel *et al.*, 1985)⁸. The strong internal tidal current with an amplitude of about 30 cm s^{-1} was observed 4 m above the sea bottom (water depth of

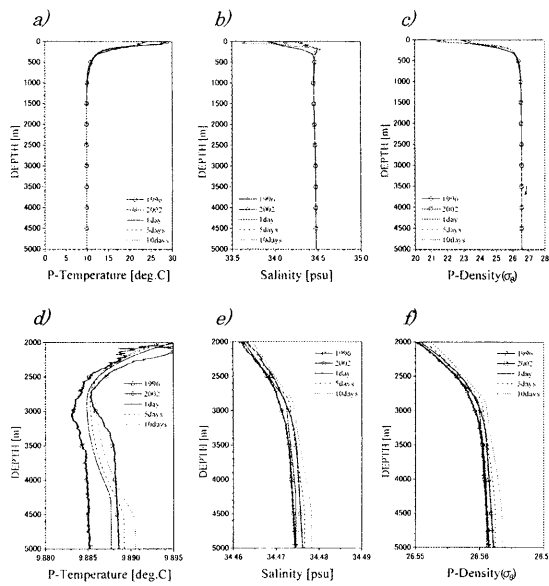


Fig.11 Comparison between observed and calculated vertical profiles of potential water temperature (a), salinity (b), and potential density (c), and those in the part deeper than 2,000 m (d), (e) and (f), respectively.

1,370 m) in the Suruga Trough, Japan, due to the propagation of internal wave energy from the upper layer (Matsuyama *et al.*, 1993)⁹⁾.

The subducted water mass volume across the 2,000 m depth of the Sulu Sea was $4.0 \times 10^{10} \text{ m}^3$ in the case of 5 days supply of heavy water mass at 400 m depth in the South China Sea from our calculated results. This means that the average residence time of the deep water below 2,000 m by such subduction is estimated to be 1.1×10^5 years; $7.5 \times 10^{14} \text{ m}^3$ (volume of the deep water below 2,000 m) / $(4.0 \times 10^{10} \text{ m}^3 / 6 \text{ years})$ (subducted water mass flux). This result is completely different from the average residence time of the deep water in the Sulu Sea (300 ± 150 years) estimated from the chemical tracer (Nozaki *et al.*, 1999)²⁾. However, the vertical diffusion time of the deep water below 2,000 m in the Sulu Sea by a large vertical diffusivity of $10 \text{ cm}^2 \text{ s}^{-1}$ is 285 years $((3,000 \text{ m})^2 / 10 \text{ cm}^2 \text{ s}^{-1})$. This value is nearly the same as the average residence time of 300 ± 150 years found by Nozaki *et al.* (1999)²⁾. This result suggests that the average residence time of the deep water in the Sulu Sea is mainly decided not by the subduction of heavy water mass from 400 m depth of the South China Sea but the large vertical turbulence in the deep water of the Sulu Sea due to the propagation of internal wave energy from the upper layers.

7. Conclusions

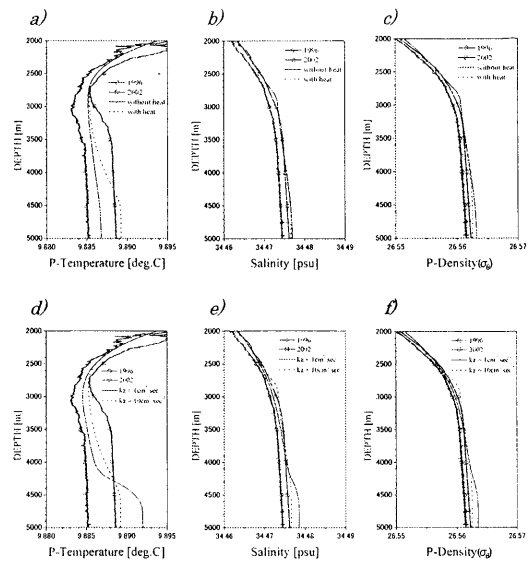


Fig.12 Comparison between observed and calculated vertical profiles of potential water temperature (a), salinity (b) and potential density (c) with terrestrial heat flow and without terrestrial heat flow, and those of potential water temperature (d), salinity (e) and potential density (f) with K_z of $10 \text{ cm}^2 \text{ s}^{-1}$ and K_z of $1 \text{ cm}^2 \text{ s}^{-1}$.

The deep water in the Sulu Sea is directly ventilated by sporadic subduction resulting from the uplifting of the heavy water mass to 400 m depth of the South China Sea due to the anti-cyclonic surface circulation near the Mindoro Strait and typhoons passing over the South China Sea in autumn. However, the average residence time of deep water in the Sulu Sea (as long as about 300 years) is not mainly decided by the subduction of heavy water mass, but the large vertical turbulence due to the propagation of internal wave energy from the upper layers. The direct measurement of turbulence using the current shear profiler is necessary near the bottom of the Sulu Sea.

We will reproduce the change in DO profiles in the Sulu Sea by another numerical experiment including the biogeochemical process in the near future.

Acknowledgements

The authors appreciate Dr.M.Shimizu, who drew Figs.2 (b) - (e). This study was supported by the Japan Society for the Promotion of Sciences.

References

- 1) Quadfasel, D., H. Kudrass and A. Frische (1990): Deep-water renewal by turbidity currents in the Sulu Sea. *Nature*, 348, 320-322.

- 2) Nozaki, Y., D.S. Alibo, H. Amakawa, T. Gamo and H. Hasumoto (1999): Dissolved rare earth elements and hydrography in the Sulu Sea. *Geochimica et Cosmochimica Acta*, 63, 2, 171-2, 181.
- 3) Morimoto, A., K. Yoshimoto and T. Yanagi (2000): Characteristics of sea surface circulation and eddy field in the South China Sea revealed by satellite altimetric data. *J. Oceanogr.*, 56, 331-344.
- 4) Gamo, T. K. Hasumoto, Y. Kato, H. Kakiuchi and N. Momoshima (2003): Water mass structure and circulation in the Sulu Sea from the chemical tracer distributions. Proceedings of the Spring Meeting of Oceanographic Society of Japan, 184.
- 5) Hinz, K. and M. Block (1990): Summary of geophysical data from the Sulu and Celebes Seas. Proceedings of the Ocean Drilling Program, ed. by C. Rangin *et al.*, 87-92.
- 6) Lewis, S. D. (1991): Geophysical setting of the Sulu and Celebes Seas. Proceedings of the Ocean Drilling Program, Scientific Results, 124, 65-71.
- 7) Blunberg, A.F. and G.L. Mellor (1987): A description of a three dimensional coastal ocean circulation model. Three-dimensional coastal ocean models, Coastal and Estuarine Sciences, Vol.4, ed. by N. Heaps, Americ. Geophys. Union, 1-16.
- 8) Apel, J.R., J.R. Holbrook, K.L. Antony and J.J. Tsai (1985): The Sulu Sea internal soliton experiment. *J. Phys. Oceanogr.*, 15, 1, 625-1, 651.
- 9) Matsuyama, M., S. Ohta, T. Hibiya and H. Yamada (1993): Strong tidal currents observed near the bottom in the Suruga Trough, central Japan. *J. Oceanogr.*, 49, 683-696.